

Polariton Condensation in an optically induced 2D potential

A. Askitopoulos,^{1,*} H. Ohadi,¹ A.V. Kavokin,^{1,2} Z. Hatzopoulos,^{3,4} P.G. Savvidis,^{3,5} and P.G. Lagoudakis¹

¹*School of Physics and Astronomy, University of Southampton, Southampton, SO17 1BJ, United Kingdom*

²*Spin Optics Laboratory, St-Petersburg State University, 1, Ulianovskaya, St-Petersburg, 198504, Russia*

³*Microelectronics Research Group, IESL-FORTH, P.O. Box 1527, 71110 Heraklion, Crete, Greece*

⁴*Department of Physics, University of Crete, 71003 Heraklion, Crete, Greece*

⁵*Department of Materials Science and Technology, University of Crete, Crete, Greece*

We demonstrate experimentally the condensation of exciton-polaritons through optical trapping. The non-resonant pump profile is shaped into a ring and projected to a high quality factor microcavity where it forms a 2D repulsive optical potential originating from the interactions of polaritons with the excitonic reservoir. Increasing the population of particles in the trap eventually leads to the emergence of a confined polariton condensate that is spatially decoupled from the decoherence inducing reservoir, before any build up of coherence on the excitation region. In a reference experiment, where the trapping mechanism is switched off by changing the excitation intensity profile, polariton condensation takes place for excitation densities more than two times higher and the resulting condensate is subject to a much stronger dephasing and depletion processes.

Strong coupling of cavity photons and quantum-well excitons gives rise to mixed light-matter bosonic quasi-particles called exciton-polaritons or polaritons [1]. Due to their photonic component, polaritons are several orders of magnitude lighter than atoms, which makes their condensation attainable at higher temperatures [2, 3]. The manifestations of polariton condensation include polariton lasing [4], long-range spatial coherence [5, 6] and stochastic vector polarisation [7]. In an ideal infinite two-dimensional cavity the polariton gas is expected to undergo the Berezinsky-Kosterlitz-Thouless (BKT) phase transition [8], while in realistic structures, polaritons can condense in traps induced by random optical disorder [2] or mechanically created potentials [3, 9]. Polariton condensation has also been observed in structures of lower dimensionality [10–13] where the structure itself acts as the trapping potential. Furthermore, the manipulation of polariton condensates by optically generated potentials has been previously shown [14–16]. In these works the condensation process was not assisted by the optical potential but used to localize an already formed polariton condensate.

Here, we report on the first manifestation of polariton condensation assisted by an optically generated two dimensional potential. This scheme allows for the formation of a polariton condensate spatially separated from the excitation spot. Owing to the efficient trapping in the optical potential we observe a reduced excitation density threshold as well as higher coherence due to the decoupling of the condensate from the exciton reservoir. Polariton condensation prior to the build-up of coherence in the form of photon or polariton lasing [17, 18] at the excitation area on the sample, decisively resolves the debate on the phase relation between the excitation laser and polariton condensate.

We used a high quality factor GaAs/AlGaAs microcavity containing four separate triplets of 10 nm GaAs quantum wells and has a vacuum Rabi splitting of 9 meV [19],

held at ~ 6.5 K in a cold-finger cryostat and excited non-resonantly at the first reflection minimum above the cavity stop band with a single-mode continuous wave laser. The excitation beam profile was shaped into a ring in real space with the use of two axicons and was projected to the microcavity through an objective lens (NA = 0.4) creating a polariton ring with a mean diameter of $\sim 20 \mu\text{m}$ on the sample (Supplementary Information, ??), which is of the order of the polariton mean free path in planar microcavities and much larger than the exciton diffusion length of the quantum wells of our sample [20, 21]. The excitation beam intensity was modulated with an acousto-optic modulator at 1% duty cycle with a frequency of 10 kHz to reduce heating.

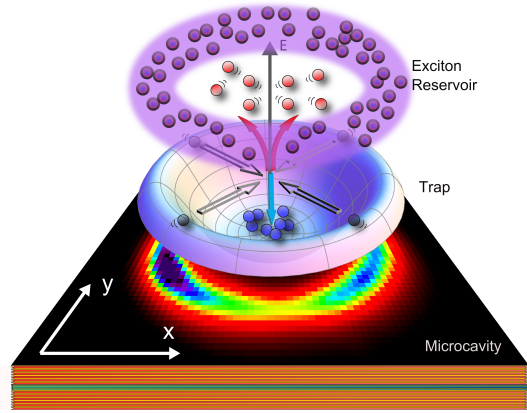


FIG. 1. Polariton trap over real space excitation spot, displaying the trapping mechanism. Polaritons scattered to high energy states leave the trap, while those scattered to low energy and momentum remain confined.

The nonresonant excitation creates a hot electron-hole plasma, which then forms excitons. Hot excitons cool down by exciton-phonon scatterings [22]. When they enter the light cone they couple strongly to the cavity mode and populate the lower polariton branch on the ring. Ex-

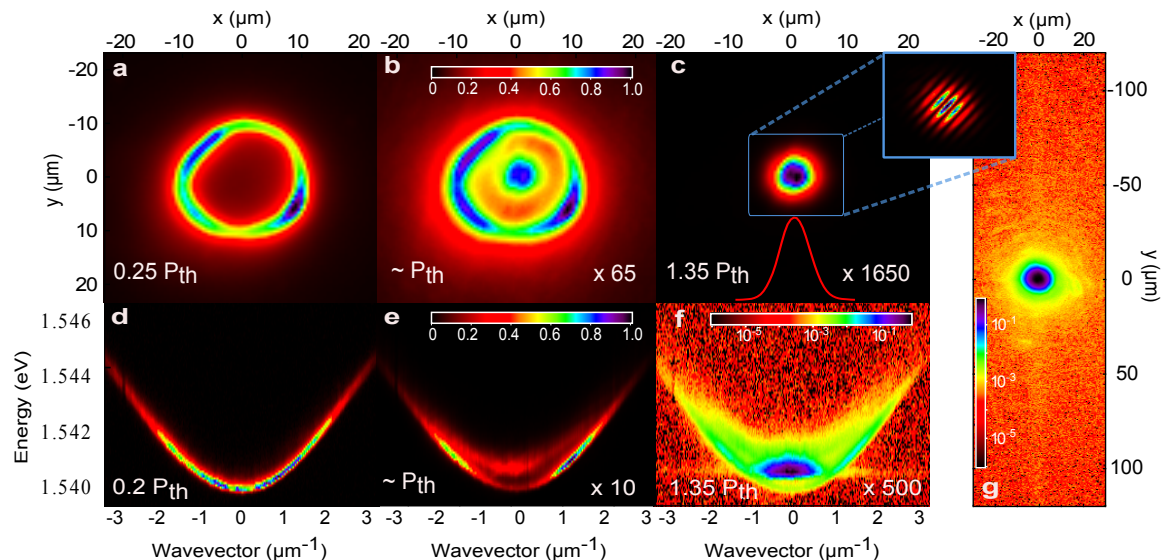


FIG. 2. Single-mode exciton-polariton condensate in a ring-shaped trap. Emission images in real space below (a), at (b) and above threshold (c). The inset in (c) shows the interference fringes of the condensate. Red line in (c) is the condensate profile along the x axis. Polariton condensation is clearly visible in the center of the ring and is separate from the excitation spot outlined by the emission in (a). (d), (e), (f) Dispersion images below (d), at (e) and above (f) threshold. (g), Same as (c) but with a logarithmic colourscale showing that the condensate propagation beyond the trap is minimal.

citons diffuse around the excitation area but due to their large effective mass they are unable to reach the center of the ring. The repulsion of polaritons from the ring-shaped exciton reservoir can be described by a mean-field ring-like trapping potential, which is approximately 1 meV deep in the center at the pumping power corresponding to the condensation threshold. Uncondensed polaritons start from the blueshifted states on the ring and ballistically expand [23] either towards the center or outside. Those which propagate to the center eventually collide with each other (see Fig 1). The energy of the ensemble of polaritons is conserved by these scattering events, so that the kinetic energies of approximately half of the polaritons are reduced, while the other half have their kinetic energies increased. As a result, a fraction of the polariton gas is no more capable to escape from the trap due to the lack of kinetic energy, while the rest can easily fly away over the barriers. Further scatterings of the trapped polaritons lead to the increase of the kinetic energy of some of them so that they become able to leave the trap. By increasing the excitation power, the polariton population inside the trap builds up and a condensate forms at the center of the ring that is quickly enhanced due to final state polariton stimulated scatterings [24].

Polariton emission in real space for powers greatly below threshold outlines the pump profile (Fig. 2a). At the onset of condensation, photoluminescence (PL) from the center of the trap is of the same intensity as emission from the ring (Fig. 2b). Above threshold (Fig. 2c,g) a Gaussian shaped single-mode condensate, with full width at half maximum (FWHM) of $5.46 \mu\text{m}$ and standard de-

viation $\sigma_x = 2.32 \mu\text{m}$, is formed and effectively confined inside the ring (images of the complete power dependence have been compiled in a video that can be found in the supplementary information). Michelson interferometry images (inset in Fig. 2c) confirm the buildup of coherence in the condensate (Supplementary Information, ??).

The dispersion of polaritons for the entire surface of the ring and for different pumping powers can be seen at Fig. 2d-f. Below threshold we observe a normal parabolic lower polariton branch. As the polariton density in the centre of the ring is increased close to threshold, we observe a blueshifted dispersion from the polaritons in the trap, coexisting with the parabolic dispersion of untrapped polaritons as it will become evident further on in this Communication from spatially resolved dispersion imaging. The two lobes of the outer dispersion in Fig. 2e correspond to high momentum polaritons escaping from the centre of the ring. By further increasing the excitation power a condensate appears in the ground state of the blueshifted dispersion with zero in-plane momentum and standard deviation $\sigma_{k_x} = 0.24 \mu\text{m}^{-1}$, shown in logarithmic scale in Fig. 2f. The macroscopically occupied ground state is very close to the Heisenberg limit, having $\sigma_x \sigma_{k_x} = 0.56$ lower than previously reported values [25]. This confirms that phase fluctuations in the condensate are strongly reduced.

Spatially-resolved dispersion images reveal that untrapped polaritons positioned on the rim of the ring have high energies and large wavevectors (Fig. 3b), while those in the center of the trap primarily populate the lower states even at pump powers much below threshold

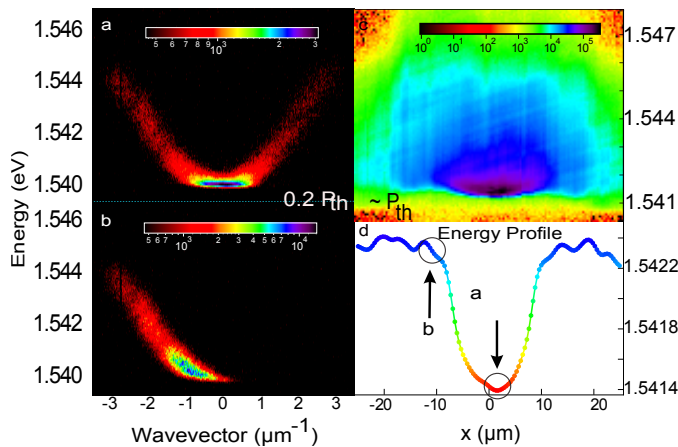


FIG. 3. Trapping potential and spatially-resolved dispersions. (a), (b), Dispersion images below threshold ($P = 0.2P_{th}$) from a $5\mu\text{m}$ diameter spatially filtered region from the center of the ring (a) and from the rim (b). Energy profile of the central slice of the ring at threshold (c) and the extracted maxima of intensity along the x axis for visualization of the trap profile (d). Points a and b correspond to (a) and (b) respectively.

(Fig. 3a) (see also supplementary information ??). The dispersion of the polaritons on the edge of the ring does not change greatly with increasing power (for the power range that we examined), while the dispersion images at the center of the trap demonstrate condensation at $k = 0$ above threshold. The profile of the trap can be visualized by energy resolving the central slice ($< 0.2\mu\text{m}$) of the excitation ring (Fig. 3c). By extracting the energy that corresponds to the maximum intensity along each point of the x axis of Fig. 3c, the trap potential can be assembled (Fig. 3d). The trap depth at threshold is $\sim 1\text{meV}$. The two circles in Fig. 3d annotate the points where the spatially filtered dispersions were acquired.

Full spatial separation of the condensate from the pump induced excitonic reservoir has important implications on the spectral and dynamic properties of polaritons [26] even below threshold. Due to the efficient stimulated scattering process we observe lower power densities for condensation. In a reference experiment we have excited the same sample (at the same detuning and temperature) with a normal Gaussian beam of spot size of $\sim 5\mu\text{m}$. Fig. 4a shows the integrated PL peak intensity of $k = 0$ for different excitation powers. The threshold power density is more than two times higher in the case of Gaussian excitation.

A clear advantage of separation of the condensate from the feeding reservoir is in the strong reduction of the depletion processes caused by condensate-reservoir interactions [27]. Fig. 4b shows the linewidth and blueshift of the condensate for the ring and Gaussian excitation cases. Due to the absence of decoherence mechanisms by the background reservoir in the case of ring-excitation, the

linewidth is narrower and it increases much slower than in the Gaussian excitation. In the case of the ring excitation the dephasing of the condensate due to the interaction with the exciton reservoir is strongly suppressed [28]. The blueshift of the condensate increases linearly with the pumping intensity, in the case of ring-like excitation, showing the linear increase of the mean number of condensed polaritons. In the case of Gaussian excitation, the blue shift is strongly affected by the reservoir: it is twice as large as in the ring-excitation case and slowly saturates above threshold, indicating that exciton saturation has been reached [29].

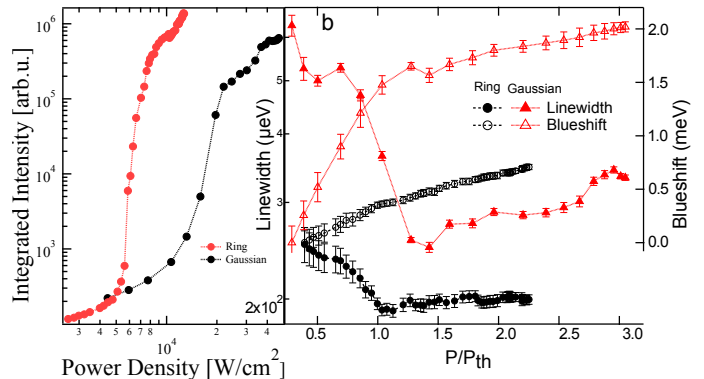


FIG. 4. Normalized intensity, linewidth and blueshift. (a), Normalized intensity with increasing power density for polaritons in the center (open black dots) of the ring excitation, and for a Gaussian excitation (open red circles) measured at $k=0 \pm 0.05\mu\text{m}^{-1}$ of the spatially filtered dispersion. (b), Linewidth (in log scale) and blueshift (right axis) vs. excitation power for polaritons at the center of the ring (black circles, open black circles respectively) and a Gaussian excitation (red triangles, open red triangles respectively). Lines are guides for the eyes.

In conclusion, we have demonstrated the condensation of a polariton bosonic gas in a two-dimensional optical trap. This configuration allows for the formation of a polariton condensate spatially separated from the excitation area minimizing dephasing and depletion processes associated with the excitonic reservoir. This highly efficient excitation technique of exciton-polaritons results in the spontaneous formation of a polariton BEC spatially separated from the excitation laser and at more than two times lower excitation densities compared to previous experimental configurations. In the case of a polariton BEC formed through optical trapping the linewidth reduces and clamps at threshold clearly evidencing that temporal coherence is not affected by increasing the occupation number of the condensate. Disassociation of the condensate from the excitation beam, conclusively settles the debate on the inheritance of coherence of the polariton condensate from the excitation laser.

We acknowledge funding from Marie Curie ITNs Spinoptronics, Clermont IV and EPSRC through Con-

tract No. EP/F026455/1. P.G.S. acknowledges funding from the EU Social Fund and Greek National Resources (EPEAEK II, HRAKLEITOS II).

* correspondence address: A.Askitopoulos@soton.ac.uk

- [1] A. V. Kavokin, J. Baumberg, G. Malpuech, and F. P. Laussy, *Microcavities* (Oxford Univ. Press, Oxford, 2007).
- [2] J. Kasprzak, M. Richard, S. Kundermann, A. Baas, P. Jeambrun, J. M. J. Keeling, F. M. Marchetti, M. H. Szymańska, R. André, J. L. Staehli, V. Savona, P. B. Littlewood, B. Deveaud, and L. S. Dang, *Nature* **443**, 409–14 (2006).
- [3] R. Balili, V. Hartwell, D. Snoke, L. Pfeiffer, and K. West, *Science* **316**, 1007 (2007).
- [4] S. Christopoulos, G. B. H. von Högersthal, A. J. D. Grundy, P. G. Lagoudakis, A. V. Kavokin, J. J. Baumberg, G. Christmann, R. Butté, E. Feltin, J.-F. Carlin, and N. Grandjean, *Physical Review Letters* **98**, 126405 (2007).
- [5] G. Nardin, K. G. Lagoudakis, M. Wouters, M. Richard, A. Baas, R. André, L. S. Dang, B. Pietka, and B. Deveaud-Plédran, *Physical Review Letters* **103**, 256402 (2009).
- [6] H. Deng, G. S. Solomon, R. Hey, K. H. Ploog, and Y. Yamamoto, *Physical Review Letters* **99**, 126403 (2007).
- [7] H. Ohadi, E. Kammann, T. C. H. Liew, K. G. Lagoudakis, A. V. Kavokin, and P. G. Lagoudakis, *Physical Review Letters* **109**, 016404 (2012).
- [8] G. Malpuech, Y. G. Rubo, F. P. Laussy, P. Bigenwald, and A. V. Kavokin, *Semiconductor Science and Technology* **18**, S395 (2003).
- [9] R. B. Balili, D. W. Snoke, L. Pfeiffer, and K. West, *Applied Physics Letters* **88**, 031110 (2006).
- [10] M. Maragkou, A. J. D. Grundy, E. Wertz, A. Lemaître, I. Sagnes, P. Senellart, J. Bloch, and P. G. Lagoudakis, *Physical Review B* **81**, 081307 (2010).
- [11] D. Bajoni, P. Senellart, E. Wertz, I. Sagnes, A. Miard, A. Lemaître, and J. Bloch, *Physical Review Letters* **100**, 047401 (2008).
- [12] L. Ferrier, E. Wertz, R. Johne, D. D. Solnyshkov, P. Senellart, I. Sagnes, A. Lemaître, G. Malpuech, and J. Bloch, *Physical Review Letters* **106**, 126401 (2011).
- [13] A. Das, P. Bhattacharya, J. Heo, A. Banerjee, and W. Guo, *Proceedings of the National Academy of Sciences* **110**, 2735 (2013), PMID: 23382183.
- [14] E. Wertz, L. Ferrier, D. D. Solnyshkov, R. Johne, D. Sanvitto, A. Lemaître, I. Sagnes, R. Grousson, A. V. Kavokin, P. Senellart, G. Malpuech, and J. Bloch, *Nature Physics* **6**, 860 (2010).
- [15] G. Tosi, G. Christmann, N. G. Berloff, P. Tsotsis, T. Gao, Z. Hatzopoulos, P. G. Savvidis, and J. J. Baumberg, *Nat Phys advance online publication* (2012), [10.1038/nphys2182](https://doi.org/10.1038/nphys2182).
- [16] T. Gao, P. S. Eldridge, T. C. H. Liew, S. I. Tsintzos, G. Stavrinidis, G. Deligeorgis, Z. Hatzopoulos, and P. G. Savvidis, *Physical Review B* **85**, 235102 (2012).
- [17] E. Kammann, H. Ohadi, M. Maragkou, A. V. Kavokin, and P. G. Lagoudakis, *New Journal of Physics* **14**, 105003 (2012).
- [18] H. Deng, G. Weihs, D. Snoke, J. Bloch, and Y. Yamamoto, *Proceedings of the National Academy of Sciences* **100**, 15318 (2003), PMID: 14673089.
- [19] P. Tsotsis, P. S. Eldridge, T. Gao, S. I. Tsintzos, Z. Hatzopoulos, and P. G. Savvidis, *New Journal of Physics* **14**, 023060 (2012).
- [20] W. Heller, A. Filoramo, P. Roussignol, and U. Bockelmann, *Solid-State Electronics* **40**, 725 (1996).
- [21] Y. Nagamune, H. Watabe, F. Sogawa, and Y. Arakawa, *Applied Physics Letters* **67**, 1535 (1995).
- [22] M. Gulia, F. Rossi, E. Molinari, P. E. Selbmann, and P. Lugli, *Physical Review B* **55**, R16049 (1997).
- [23] E. Kammann, T. C. H. Liew, H. Ohadi, P. Cilibrizzi, P. Tsotsis, Z. Hatzopoulos, P. G. Savvidis, A. V. Kavokin, and P. G. Lagoudakis, *Physical Review Letters* **109**, 036404 (2012).
- [24] P. G. Savvidis, J. J. Baumberg, R. M. Stevenson, M. S. Skolnick, D. M. Whittaker, and J. S. Roberts, *Physical Review Letters* **84**, 1547 (2000).
- [25] G. Roumpos, W. H. Nitsche, S. Höfling, A. Forchel, and Y. Yamamoto, *Physical Review Letters* **104**, 126403 (2010).
- [26] D. V. Vishnevsky, D. D. Solnyshkov, N. A. Gippius, and G. Malpuech, *Physical Review B* **85**, 155328 (2012).
- [27] A. P. D. Love, D. N. Krizhanovskii, D. M. Whittaker, R. Bouchekioua, D. Sanvitto, S. A. Rizeiqi, R. Bradley, M. S. Skolnick, P. R. Eastham, R. André, and L. S. Dang, *Physical Review Letters* **101**, 067404 (2008).
- [28] D. Porras and C. Tejedor, *Physical Review B* **67**, 161310 (2003).
- [29] T. M. Holden, G. T. Kennedy, A. R. Cameron, P. Riblet, and A. Miller, *Applied Physics Letters* **71**, 936 (1997).